

Phosphorous-doped porous carbon derived from paste of newly growing *Ficus benghalensis* as hydrogen storage material

Arjunan Ariharan, Balasubramanian Viswanathan* & Vaiyapuri Nandhakumar
National Centre for Catalysis Research, Indian Institute of Technology Madras, Chennai 600 036, India
Email: bvnathan@iitm.ac.in

Received 28 February 2016; revised and accepted 26 May 2016

The synthesis of heteroatom (P)-doped porous carbon derived from the paste of newly growing Indian banyan tree (*Ficus benghalensis*) is described. The synthesis involves activation, carbonization and phosphorous-doping processes using H_3PO_4 as activating agent and as phosphorous source. The phosphorous-doped porous carbon material shows a wafer-like morphology with specific surface area of 1406 m^2/g . This material exhibits hydrogen storage capacity of ~1.2 wt% at 298 K and 100 bar. This easily prepared carbon material is promising for realistic hydrogen storage.

Keywords: Hydrogen storage, Carbon materials, Porous carbon, Activation, Biomass, Heteroatom doped carbon, Phosphorous doped carbon, *Ficus benghalensis*

In recent years, renewable energy and environmental protection have been the two main concerns of research. The missing connection in the hydrogen based economy is storage. For the hydrogen based economy to become feasible, breaking points on hydrogen storage capacity, reversibility and cost viability are the necessary conditions. Specifically, building up a sheltered and productive hydrogen storage system at room temperature and atmospheric pressure is significantly difficult and challenging¹. Compressed gas, cryogenic liquid tanks, and hydrogen storage materials, such as metal hydride, chemical hydride, metal organic frameworks, and adsorbed materials are the general choices for the hydrogen storage community¹⁻⁴. The established hydrogen-storage systems are difficult because of its low boiling point and low density in the gaseous state. Liquid hydrogen requires the addition of a refrigeration unit to sustain a cryogenic condition, thereby adding up weight and energy expenses^{5,6}. The materials for hydrogen storage show the ill effects of poor adsorption/desorption reversibility, intrinsic moderate energy, thermodynamic energy inefficiency, optional pollution brought on by the response items and high expenses of production and recovery^{1,4}.

In this energy scene, nanostructured carbon materials have received consideration as materials suitable for hydrogen storage⁷. On the other hand, till

now, the required hydrogen storage capacity limit according to DOE specifications for FY 2005 (4.5 wt%), FY 2010 (6 wt%) and 9 wt% for FY 2015, has not been accomplished despite the fact that impressive endeavors have been put to achieve this goal⁸. Hydrogen storage in carbon materials has received consideration following the report of storage capacity (however surprisingly high) of around 67 wt% was reported by Chambers et al^{9,10}. Hydrogen sorption on carbonaceous materials like carbon nanotubes^{11,12}, fullerenes¹³⁻¹⁴, carbon nanofibers^{15,16}, graphite nanofibers⁹, activated carbons^{17,18}, graphene² and graphite¹⁹ has been examined. The porous carbon materials are particularly encouraging in light of the fact that they are cost effective and facile to synthesis^{20,21}. They have prevalent chemical, thermal, and mechanical stability, their porous structure is effectively planned and easy to recover. Precursors utilized for the synthesis of porous carbons, derived from renewable biomass and biomass waste, are straw and sawdust²², dead mango leaves²³, banana-stem²⁴, coconut shell²⁵, corn husks²⁶ and soya chunks²⁷. These materials have been used for hydrogen storage, electrochemical energy storage, electrochemical determination, CO₂ capture, super capacitor and oxygen reduction applications²⁸⁻³¹. In addition, these carbon materials can be doped with the heteroatoms like nitrogen, phosphorous, boron and sulfur, which might improve H₂ adsorption by presenting active

sites^{4,32-35}. This inexpensive and accessible carbon material can be used to dope phosphorous for hydrogen storage purposes³⁶.

The synthesis method for the heteroatom-substituted carbon materials is through carbonization of heteroatom and carbon containing precursors followed by additional physical and chemical activation^{5-6,37}. The large scale synthesis of phosphorous-doped porous carbons, starting from biomass under various preparation conditions, is an attractive one as a source material to enhance hydrogen storage capacity. However, the heteroatom (P) doped carbon materials are prepared from carbonization, followed by H_3PO_4 activation³⁸⁻⁴². The activation with H_3PO_4 is environment-friendly as it does not pollute, simple to recover by just solubilizing the H_3PO_4 salts in water and can be reused over into the process⁴³. In our research group previous studies, we have prepared heteroatom substituted carbon materials from pyrolyzed polymeric precursors, which confirms the high specific surface area and hydrogen sorption capacity up to ~5.9 wt % at 298 K and 100 bar^{44,45}. The point of this work is to amplify the sustainable approach towards phosphorous-doped carbon material with accentuation on the utilization of facile low-cost and bio-based precursors.

The selection of materials depends essentially on advanced hydrogen storage to meet the increasing and critical demand for the renewable energy resources. The cooperation involving the high surface area and good porous nature in carbon materials imparts enhancement of the hydrogen storage capacity.

By this route, one can without difficulty obtain porous carbon material from the paste of the new plants of the inexpensive and sustainable *Ficus benghalensis*. The synthesis of phosphorous-doped porous carbon material from the most abundant tree in india, viz., *Ficus benghalensis* (Indian banyan tree) has been described. To the best of our knowledge no report is available where *Ficus benghalensis* paste was utilized as a precursor to synthesize carbon.

Materials and Methods

Phosphoric acid (H_3PO_4) was purchased from Sigma-Aldrich. Indian banyan tree (common name) (Botanical name: *Ficus benghalensis*, Family: Moraceae) were collected from Indian Institute of Technology Madras campus Chennai (Tamilnadu, India). (In Tamil, it is known as aalamaram).

Synthesis of porous carbon

Figure 1 shows the schematic illustration of phosphorous-doped carbon material. Typical synthesis procedure is as follows: The paste of newly growing (*Ficus benghalensis*, Family: Moraceae) was collected and cut into small pieces then thoroughly washed and dried in an oven at 90 °C. The crushed pastes were impregnated with 35 mL of H_3PO_4 for 24 h and dried in sunlight for 6 h to remove the moisture. For the activation process, the preferred amount of preheated crushed paste was transferred in a quartz boat kept at center of the tubular furnace. To optimize the activation temperature, the furnace was initially heated at 200 °C and then the heating was continued at 800 °C under N_2 atmosphere at the heating

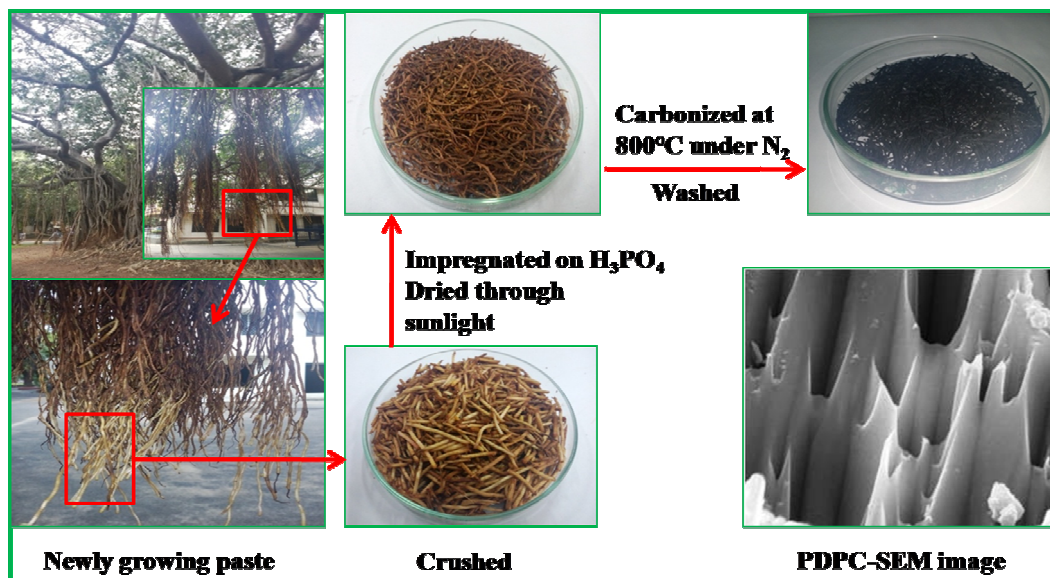


Fig. 1—The schematic preparation method of phosphorous-doped porous carbon material.

rate of 5 °C/min. After the calcination, the tubular furnace was cooled to room temperature. The calcined material was washed with distilled water thoroughly. Then, the samples were dried at 90 °C overnight to remove any moisture. The resulting carbon material was ground into a fine powder using a mortar and pestle. The material was then transferred to a cintillation vial for storage. Finally, the synthesized phosphorous-doped porous carbon (PDPC) material was utilized for further characterization. A similar synthesis method was adopted to prepare the pure carbon material without phosphorous.

Physical characterization

Wide angle powder XRD pattern of the calcined carbon materials was recorded using a Rigaku Miniflex II diffractometer with Cu K α as the radiation source at a wavelength of 0.154 nm and 2 θ angle ranging from 10° to 80° with a 0.02 step size. Fourier transform infrared spectra (Perkin-Elmer FTIR spectrophotometer) were collected at room temperature by using the KBr pellet technique working in the wave numbers range of 4000–400 cm⁻¹. Fourier transform Raman spectra were recorded by using the standard Bruker pulse FT-Raman spectrometer instrument. BET N₂ adsorption and desorption isotherms were measured with surface area and porosity analyzer (Micromeritics Accelerated Surface Area and Porosimetry System, ASAP 2020) for the determination of surface area and total pore volume at 77 K. Prior to the adsorption measurements, the sample was degassed at 473 K for 6 h. FEI Quanta FEG 200-High resolution scanning electron microscope was employed for obtaining the HRSEM micrographs. A JEOL JEM-2000 High resolution transmission electron microscope was employed for obtaining the HRTEM micrographs. X-ray photoelectron spectroscopy (XPS) measurements were performed with an Omicron Nanotechnology spectrometer with hemispherical analyzer. The monochromatized Mg K α X-source ($E = 1253.6$ eV) was operated at 15 kV and 20 mA. For the narrow scans, the analyzer pass energy of 25 eV was applied. The base pressure in the analysis chamber is 5×10^{-10} Torr. The hydrogen adsorption isotherms were carried out on high pressure volumetric analyzer (HPVA-100) from micromeritics particulate systems. The HPVA product operating pressure ranges from high vacuum to 100 bar. The span of the sample temperature during analysis was from cryogenic to 500 °C. Sample analysis data collection was fully automated to assure quality data and high reproducibility.

Results and Discussion

X-ray diffraction patterns

The X-ray diffraction pattern of the phosphorous-doped porous carbon material is shown in Fig. 2. Two broad peaks around 23.7° and 44.2° corresponding to 002 and 100 planes respectively were observed. This reflection is assigned to the regular turbostratic carbon lattice. The (100) planes indicates the amorphous nature of the sample. The pure carbon sample showed one broad reflection around 21.6° corresponding to 002 planes, while the phosphorous-doped carbon is more amorphous. Moreover, after the doping of heteroatom (P), the peaks are shifted slightly on higher 2 θ values. This is established by the Raman spectrum of the prepared material discussed later (See Fig. 3).

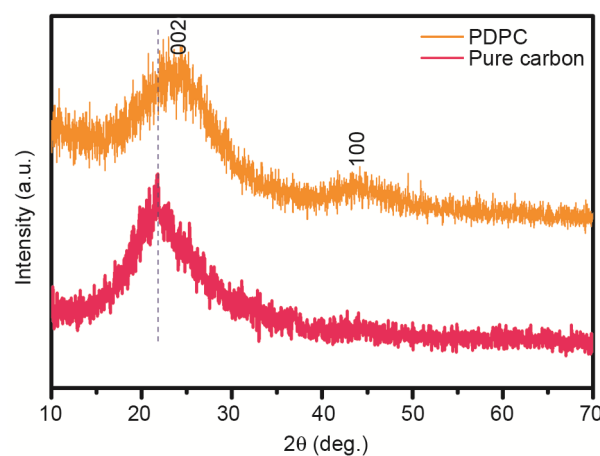


Fig. 2—X-ray diffraction patterns of the phosphorous-doped porous carbon.

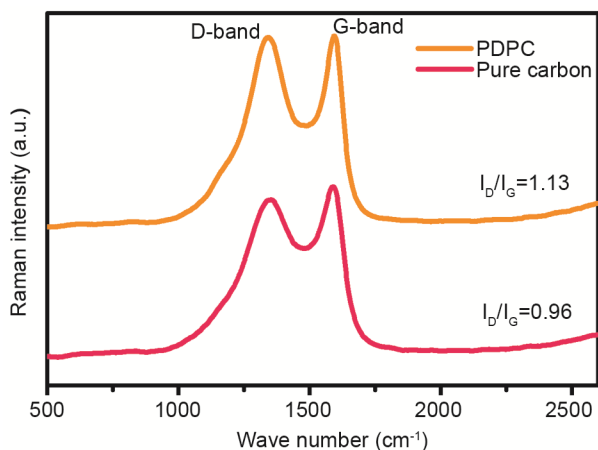


Fig. 3—Raman spectrum of the phosphorous-doped porous carbon material.

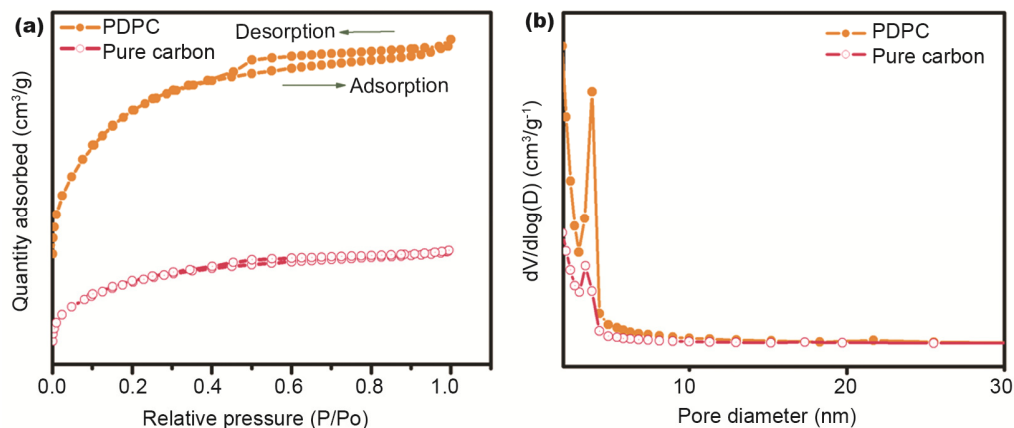


Fig. 4—Nitrogen adsorption/desorption isotherm of the phosphorous-doped porous carbon and pure carbon material.

Raman spectroscopy

The Raman spectrum of phosphorous-doped porous carbon and pure carbon materials is shown in Fig. 3. The PDPC shows two broad characteristic peaks at 1344 cm^{-1} and 1594 cm^{-1} and pure carbon material shows peaks at 1350 cm^{-1} and 1590 cm^{-1} ; these peaks correspond to D and G bands of the carbon material. These two bands confirm the presence of defects and graphitic nature of the carbon material³². These results reveal that after the H_3PO_4 activation, the graphitic nature of the material and degree of the defects increased. The D peak shifted to higher wave number with respect to pure carbon material. The ratio of integrated intensity (I_D/I_G) of the D and G bands can be used to estimate the defects/disorder in carbon material. The I_D/I_G values for phosphorous containing activated carbon material ($I_D/I_G = 1.13$) and pure carbon material prepared (without P) are 1.13 and 0.96, respectively. These values reveal higher concentration of structural defects in the phosphorous-doped porous carbon material. This result is also in agreement with TEM and XRD analysis.

BET- N_2 adsorption/desorption isotherms

The adsorption/desorption isotherms were measured to determine the specific surface area and the Barrot-Joyner-Halenda (BJH) method was utilized to estimate the pore volume of phosphorous-doped porous carbon material and the results are shown in Fig. 4. These isotherms reveal the presence of different pore sizes of micropores, mesopores and macropores. The isotherms are a mixture of Type I belonging to microporous carbon and Type IV distinguishing mesoporous nature²³. However this N_2 sorption showed a Type I sorption isotherm with a higher nitrogen sorption capacity, signifying the higher ultra-microporous property³². In addition, the

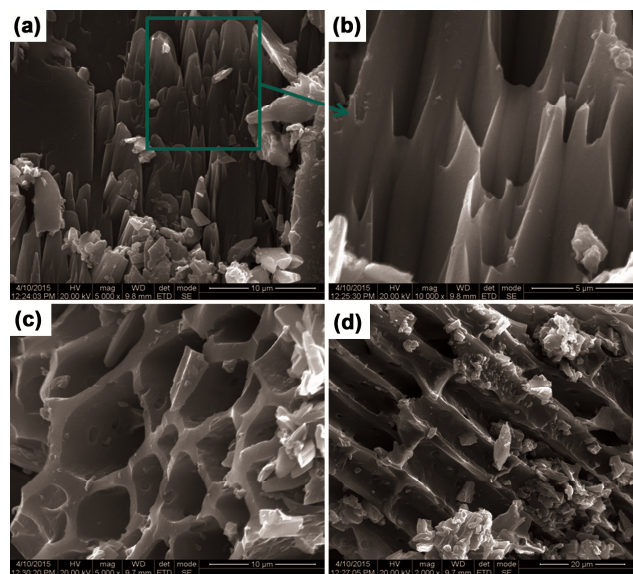


Fig. 5—HRSEM images of the phosphorous-doped porous carbon material with different magnifications.

carbon material has pore distribution peaks between 0.5 and 5 nm, which indicates the development of both micropores and small mesopores⁴⁶. The BET specific surface area values of phosphorous-doped highly porous carbon and pure carbon material are $1406\text{ m}^2/\text{g}$ and $570\text{ m}^2/\text{g}$ respectively.

High resolution scanning electron microscopy

High resolution scanning electron micrographs are shown in Fig. 5. Images in Fig. 5(a) show the array-like morphology. The same area taken to higher magnification (Fig. 5(b)) showed wafer porous array-like morphology of this material. Figure 5(c) showed the horizontal cut image of the porous arrays which will confirm its highly porous nature. Figure 5(d) shows the vertical cut of porous arrays; this image

reveals the wafer array of porous morphology of the prepared material. Furthermore, the percentage of heteroatom present in this material was analyzed by SEM-EDAX analysis. The amount of phosphorous in the carbon matrix was found to be ~2 at.% (See Fig. 7(f)).

High resolution transmission electron microscopy

The high resolution transmission electron micrographs of the phosphorous-doped porous carbon material are shown in Fig. 6. HRTEM micrographs show the array of one by one arranged porous sheets-like morphology of the prepared material (See Fig. 6a & 6b). However, Figs 6(c) & (d) show clearly a large number of micropores present in this

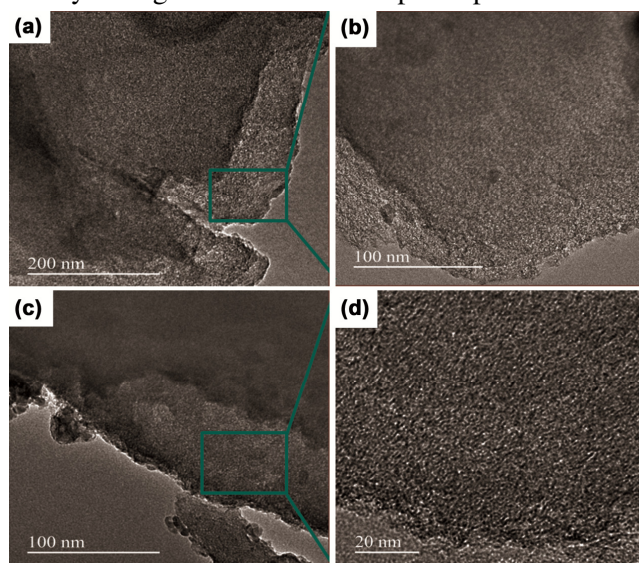


Fig. 6—HRTEM images of the phosphorous-doped porous carbon material for different magnifications.

porous carbon material. The SAED pattern of this material is shown in Fig. 7(e). The two diffraction rings represent the 002 and 100 planes and the disordered nature of the phosphorous substituted carbon material. It also confirms the existence of an amorphous composite state of carbon material and reveals a porous nature. This surveillance is in excellent conformity with the observation of HRSEM morphology analysis. Scanning TEM (STEM) with elemental mapping analysis has been carried out to authenticate the phosphorous doping in the carbon lattice and also to distinguish the homogeneity of doping. The results indicate carbon, phosphorous, and oxygen atoms present in the entire prepared material consistently (See Figs.7 (a), (b), (c) & (d)). To investigate the percentage of element present on the prepared material, HRTEM-EDAX analysis was carried out. The amount of phosphorous observed in the carbon matrix was ~2 at.% (See Fig. 7g & 7h).

Thermogravimetric analysis

Thermogravimetric analysis of the phosphorous-doped porous carbon material is shown in Fig. 8. TGA investigations provide information on the thermal stability of the carbon materials. The pure carbon material decomposes rapidly in air at an initial decomposition temperature of 400 °C, extending up till 500 °C. Interestingly, the prepared phosphorous doped porous carbon (PDPC) material exhibits higher thermal stability temperature (560 °C) which is higher than those in previous reports for other heteroatoms like N and B-doped carbon materials^{47,48}. This analysis curve showed a continuous weight loss of ~65% with a steep drop around 450 °C, which

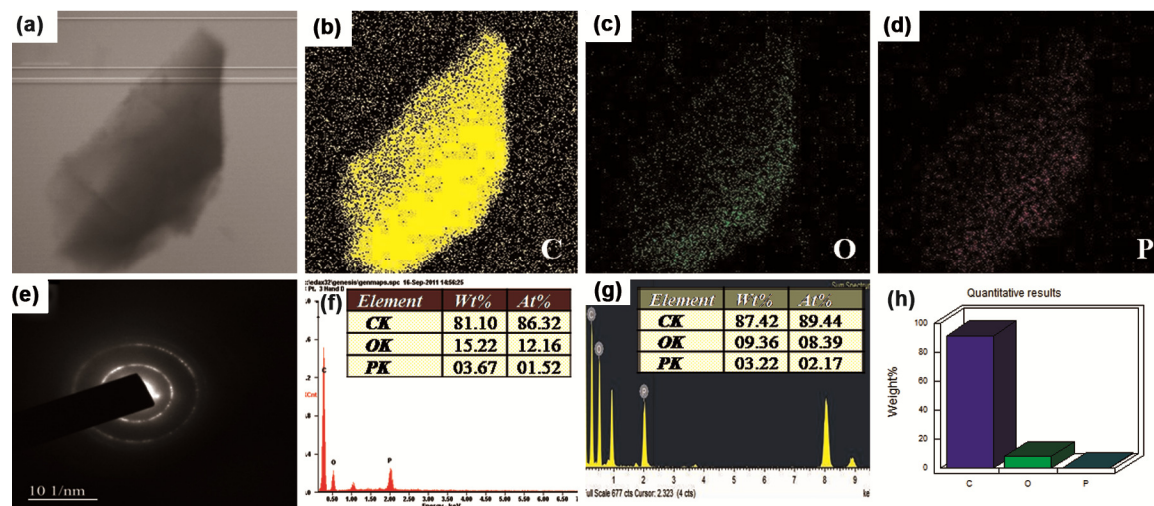


Fig. 7—(a) STEM images, (b) (c) and (d) elemental mapping images, (e) SAED pattern (f) SEM-EDAX, (g) and (h) TEM-EDAX analysis of the phosphorous-doped porous carbon material.

can be recognized as the addition of phosphoric acid. The major decomposition takes place in the temperature range 400 °C to 500 °C. However, no contaminants was observed from the carbon material after calcination at 800 °C, signifying high purity of the material without any residue^{49,50}. Finally, TGA analysis shows that the precursor from *Ficus benghalensis* can easily be changed into carbon materials with a high carbon yield, suggesting that it is a suitable precursor for preparing carbon materials.

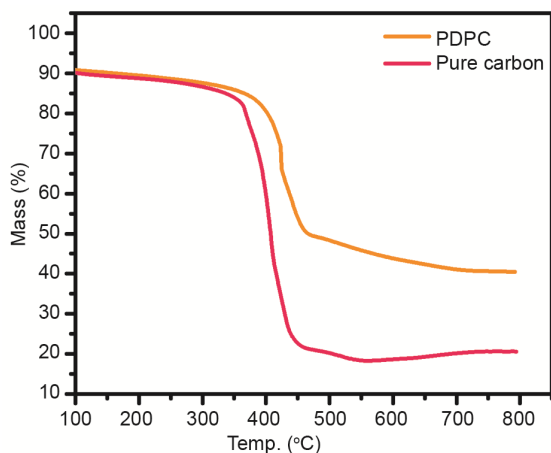


Fig. 8—TGA curves of the phosphorous-doped porous carbon material.

X-ray photoelectron spectroscopy

XPS investigation was carried out to establish the accurate amount of functional component, chemical composition and the atomic percentages of carbon, phosphorous and oxygen (Fig. 9). The XPS survey spectrum of the prepared material shown in Fig. 9(a) shows the presence of carbon, phosphorous and oxygen functionality. The carbon species showed standard 1s peaks at 284.3 eV for sp^2 -hybridized carbon bonds (C=C), 284.2 eV for sp^3 -hybridized carbon bonds (C-C), 285.2 eV for alcohol groups (C-O), carbonyl groups (C=O), 289.2 eV for carboxylic/ester groups (O-C=O)⁵³ (See Fig. 9(b)). The peaks located at 130.1 and 132.0 eV of P2p region can be assigned to the P-C and P-O/C-O-P bonding, respectively⁵¹⁻⁵⁶. The O1s peaks were deconvoluted into four components for the graphene materials (See Fig. 9(c)) The peak in the region of 532.0–532.1 eV is ascribed to oxygen double bonded to carbon (C=O) and non-bridged oxygen in the phosphate group (P=O). The peak B at BE = 533.0–532.1 eV may be assigned the total of the separately bonded oxygen in C-O and C-O-P groups respectively^{39,52,53,57}.

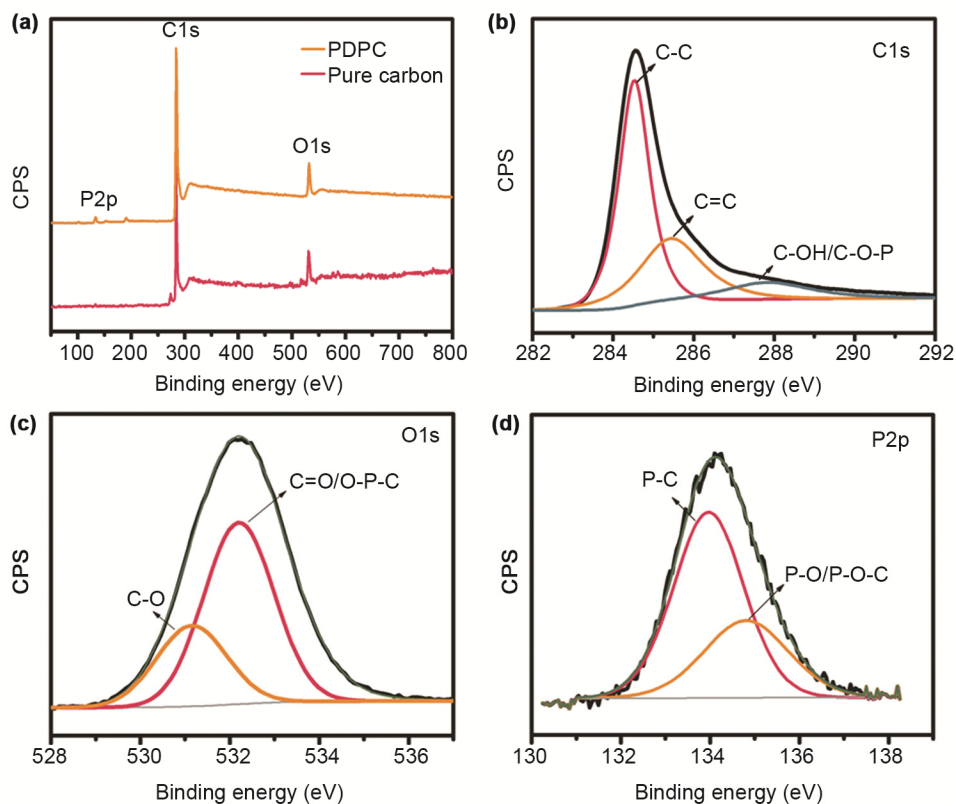


Fig. 9—X-ray photoelectron spectroscopy (XPS) of the phosphorous-doped porous carbon material.

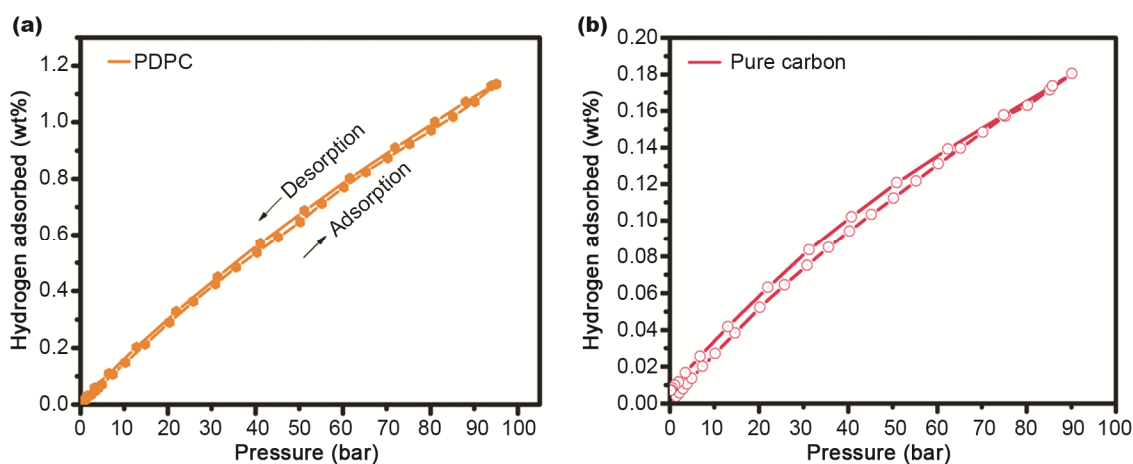


Fig. 10—Hydrogen adsorption/desorption isotherms of the phosphorous-doped porous carbon material.

Hydrogen adsorption/desorption isotherms

The hydrogen adsorption/desorption isotherm of synthesized phosphorous-doped porous carbon material is shown in Fig. 10. In phosphorus-doped carbon, the polarization induced dipole-dipole interaction (non-covalent) between H₂ and carbon material is increased due to larger charge transfer. This is expected to enhance the hydrogen adsorption for the heteroatom doped carbon materials. The hydrogen adsorption isotherm was carried out 298 K and 100 bar pressure. The phosphorous substituted graphene material showed nearly ~1.2 wt% hydrogen storage capacity at room temperature and 100 bar pressure. The undoped carbon material showed ~0.17 wt% hydrogen storage capacity at room temperature and 100 bar, which is less than that observed for the phosphorous-doped carbon material. However, while considering these aspects, heteroatoms like N, P, S and B appear to be promising as activators due to their properties like higher redox potential than that of carbon. Heteroatom substituted carbon materials show increase in the hydrogen bond length and decrease in dissociation energy as compared to unsubstituted carbon^{11,58}. Furthermore, heteroatom (P) substitution provides suitable centres for the dissociation of molecular hydrogen. Since hetero atoms take up substitutional positions in the lattice, there is facile transport of hydrogen atoms on to the carbon surface⁵⁹. Moreover, heteroatom substitution improves the sorption capacity and nearly all the adsorbed quantity is desorbed, which is an attractive feature for hydrogen storage materials.

Conclusions

The utilization of biomass or biomass wastes as precursors has been used for synthesizing porous carbon for hydrogen storage. Phosphorous-doped porous carbon material was prepared utilizing the paste of newly grown *Ficus benghalensis* (Indian banyan tree). This as-prepared porous heteroatom (P) doped carbon material showed hydrogen storage capacity of ~1.2wt% at 298 K and 100 bar. These results provide some insights into further increasing the hydrogen storage capacity in carbon materials and improving the reversibility. Thus, the proposed synthesis can be an alternative resources for P-doped porous carbon material for hydrogen adsorption.

Acknowledgement

The authors wish to record their grateful thanks to the Department of Science and Technology (DST), New Delhi, India, for supporting the National Centre for Catalysis Research, Indian Institute of Technology Madras, Chennai, India, and, Ministry New and Renewable Energy, Government of India, New Delhi, for supporting the hydrogen storage activity of this centre.

References

- 1 Jin J, Fu L, Yang H & Ouyang J, *Sci Rep*, 5 (2015) 12429.
- 2 Spyrou K, Gournis D & Rudolf P, *ECS J Solid State Sci Technol*, 2 (2013).
- 3 Jena P, *J Phys Chem Lett*, 2 (2011) 206.
- 4 Cao B, Liu H, Xing Z, Lei Y, Song H, Chen X, Zhou J & Ma Z, *ACS Sustainable Chem Eng*, 3 (2015) 1786.
- 5 Kalderis D, Bethanis S, Paraskeva P & Diamadopoulos E, *Bioresource Technol*, 99 (2008) 6809.

- 6 Liu J, Deng Y, Li X & Wang L, *ACS Sustainable Chem Eng*, 4 (2016) 177.
- 7 Candelaria S L, Shao Y, Zhou W, Li X, Xiao J, Zhang J G, Wang Y, Liu J, Li J & Cao, G, *Nano Energy*, 1 (2012) 195.
- 8 Viswanathan B, Murugesan S, Ariharan A & Lakhi K S, *Adv Por Mater*, 1 (2013) 122.
- 9 Chambers A, Park C, Baker R T K & Rodriguez N M, *J Phy Chem B*, 102 (1998) 4253.
- 10 Titirici M M, White R J, Brun N, Budarin V L, Su D S, del Monte F, Clark J H & MacLachlan M J, *Chem Soc Rev*, 44 (2015) 250.
- 11 Sankaran M & Viswanathan B, *Carbon*, 44 (2006) 2816.
- 12 He Z, Wang S, Wang X & Iqbal Z, *Int J Energ Res*, 37 (2013) 754.
- 13 Gao Y, Wu X & Zeng X C, *J Mater Chem A*, 2 (2014) 5910.
- 14 Sankaran M, Muthukumar K & Viswanathan B, *Fullerenes, Nanotubes and Carbon Nanostructures*, 13 (2005) 43.
- 15 Marella M & Tomaselli M, *Carbon*, 44 (2006) 1404.
- 16 Vázquez-Santos M B, Suárez García F, Martínez Alonso A & Tascón J M D, *Langmuir*, 28 (2012) 5850.
- 17 Blackman J M, Patrick J W, Arenilla A, Shi W & Snape C E, *Carbon*, 44 (2006) 1376.
- 18 László K, Tombácz E & Josepovits K, *Carbon*, 39 (2001) 1217.
- 19 Kumar L H, Rao C V & Viswanathan B, *J Mater Chem A*, 1 (2013) 3355.
- 20 Chen J, Yang J, Hu G, Hu X, Li Z, Shen S, Radosz M & Fan M, *ACS Sustainable Chem Eng*, 4 (2016) 1439.
- 21 Xia Y, Yang Z & Zhu Y, *J Mater Chem A*, 1 (2013) 9365.
- 22 Cheng F, Liang J, Zhao J, Tao Z & Chen J, *Chem Mater*, 20 (2008) 1889.
- 23 Madhu R, Sankar K V, Chen S M & Selvan R K, *RSC Adv*, 4 (2014) 1233.
- 24 Madhu R, Veeramani V & Chen S M, *Sci Rep*, 4 (2014) 4679.
- 25 Mohamed A. R, Mohammadi M & Darzi G N, *Renew Sust Energ Rev*, 14 (2010) 1591.
- 26 Song S, Ma F, Wu G, Ma D, Geng W & Wan J, *J Mater Chem A*, 35 (2015) 18154.
- 27 Rana M, Arora G & Gautam U K, *Sci Tech Adv Mater*, 16 (2015) 14803.
- 28 Liu F, Peng H, You C, Fu Z, Huang P, Song H & Liao S, *Electrochim Acta*, 138 (2014) 353.
- 29 Pan F, Cao Z, Zhao Q, Liang H & Zhang J, *J Power Sources*, 272 (2014) 8.
- 30 Gokhale R, Unni S M, Puthusseri D, Kurungot S & Ogale S, *Phys Chem Chem Phys*, 16 (2014) 4251.
- 31 Liu F, Peng H, Qiao X, Fu Z, Huang P & Liao S, *Int J Hydrogen Energy*, 39 (2014) 10128.
- 32 Ou J, Zhang Y, Chen L, Zhao Q, Meng Y, Guo Y & Xiao D, *Mater Chem A*, 3 (2015) 6534.
- 33 Zhu B, Shang C & Guo Z, *ACS Sustain Chem Eng*, 2016.
- 34 Lin I H, Tong Y J, Hsieh H J, Huang H W & Chen H T, *Int J Energy Res*, 40 (2016) 230.
- 35 Ting V P, Ramirez Cuesta A J, Bimbo N, Sharpe J E, Noguera Diaz A, Presser V, Rudic S & Mays T J, *ACS Nano*, 9 (2015) 8249.
- 36 Liu D, Yu S, Shen Y, Chen H, Shen Z, Zhao S, Fu S, Yu Y & Bao B, *Ind Eng Chem Res*, 54 (2015) 12570.
- 37 Hu B, Wang K, Wu L, Yu S H, Antonietti M & Titirici M M, *Adv Mater*, 22 (2010) 813.
- 38 Mopoung S & Amornsakchai P, *Asian J Sci Res*, 9 (2016) 24.
- 39 Puziy A, Poddubnaya O, Martinez Alonso A, Suárez Garcia F & Tascón J, *Carbon*, 40 (2002) 1493.
- 40 Hulicova J D, Puziy A M, Poddubnaya O I, Suárez G F, Tascón J M D & Lu G Q, *J Am Chem Soc*, 131 (2009) 5026.
- 41 Villar Rodil S, Suárez García F, Paredes J I, Martínez Alonso A, Tascón J M D, *Chem Mater*, 17 (2005) 5893.
- 42 Puziy A M, Poddubnaya O I, Martínez A A, Suárez G F & Tascón J M D, *Carbon*, 40 (2002) 1493.
- 43 Molina-Sabio M, Rodriguez Reinoso F, Caturla F & Selles M, *Carbon*, 33 (1995) 1105.
- 44 Sankaran M & Viswanathan B, *Carbon*, 45 (2007) 1628.
- 45 Ariharan A, Viswanathan B, & Nandhakumar V, *Int J Hydrogen Energy*, 41 (2016) 3536.
- 46 Li B, Dai F, Xiao Q, Yang L, Shen J, Zhang C & Cai M, *Energy Environ Sci*, 9 (2006) 102.
- 47 Singh K P, Song M Y & Yu J S, *J Mater Chem A*, 2 (2014) 18124.
- 48 Choi C H, Park S H, Chung M W & Woo S I, *Carbon*, 55 (2013) 107.
- 49 Wohlgemuth S A, Vilela F, Titirici M M & Antonietti M A, *Green Chem*, 14 (2012) 749.
- 50 Bhattacharjya D, Park H Y, Kim M S, Choi H S, Inamdar S N & Yu J S, *Langmuir*, 30 (2013) 324.
- 51 Desimoni E, Casella G I & Salvi A M, *Carbon*, 30 (1992) 52.
- 52 Puziy AM, Poddubnaya O I & Ziatdinov A M, *Appl Surf Sci*, 252 (2006) 8036.
- 53 Puziy A M, Poddubnaya O I, Socha R P, Gurgul J & Wisniewski M, *Carbon*, 46 (2008) 2113.
- 54 Li R, Wei Z & Gou X, *ACS Catal*, 5 (2015) 4133
- 55 Wen Y, Wang B, Huang C, Wang L & Hulicova J D, *Chem Eur J*, 21 (2015) 85.
- 56 Jin Z, Sun Z, Simpson L J, O'Neill K J, Parilla P A, Li Y, Stadie N P, Ahn C C, Kittrell C & Tour J M, *J. Am Chem Soc*, 132 (2010) 15246.
- 57 Poh H L, Sofer Z, Nováček M & Pumera M, *Chem Eur J*, 20 (2014) 4284.
- 58 Ariharan A, Viswanathan B & Nandhakumar V, *Indian J Chem*, 54A (2015) 1433.
- 59 Ariharan A, Viswanathan B & Nandhakumar V, *Graphene*, 5 (2016) 50.